In-Vitro Antibacterial Activity of *Piper Guineense* Extracts and their Silver Nanoparticles Against Bacterial from Gastrointestinal Tract

Bukola Christianah Adebayo-Tayo, Folarin Victor Adeola, Olusola Ademola Olaniyi & Oladeji Aderibigbe Ajani*

University of Ibadan

ABSTRACT

The study investigates the in-vitro antibacterial activity of greenly synthesized silver nanoparticles from Piper guineese leave (PgMLE) and seed (PgMSE) methanol extracts. The greenly synthesized silver nanoparticles from leave (PgMLEAgNPs) and seed (PgMSEAgNPs) extracts were characterized using UV-visible spectroscopy, FTIR, SEM, TEM, XRD, EDX, and TGA, and the in-vitro antibacterial activity of the extracts and nanoparticles against test pathogens from gastrointestinal tracts was evaluated. The PgMLE and PgMSE bio-reduced silver nitrate solution for the biosynthesis of PgMLEAgNPs and PgMSEAgNPs. The nanoparticles had the highest Surface plasmon resonance peaks at 500 nm. Functional groups such as alcohols, phenols, alkenes or alkynes, nitriles, ketones, aldehydes, or esters were identified as indicative of biomolecules present within PgMLEAgNPs, and PgMSEAgNPs. PgMLEAgNPs and PgMSEAgNPs were spherical flakelike and aggregated particles respectively with 15 nm in size, TEM shows the spherical shape nanoparticles. The nanoparticles were crystalline in nature and silver had the highest intensity as shown by XRD and EDX analysis. PgMLEAgNPs and PgMSEAgNPs exhibited varied antibacterial activity against the test pathogens.

Keywords: Piper guineense methanol extracts, antibacterial activity, Silver nanoparticles, Gastrointestinal Tracts, Pathogens.

Classification: FoR Code: 1108

Language: English

Great Britain Journals Press

LJP Copyright ID: 925621
Print ISSN: 2631-8490
Online ISSN: 2631-8504

London Journal of Research in Science: Natural and Formal

Volume 24 | Issue 4 | Compilation 1.0

In-Vitro Antibacterial Activity of *Piper Guineense* Extracts and their Silver Nanoparticles Against Bacterial from Gastrointestinal Tract

Bukola Christianah Adebayo-Tayo[α] *, Folarin Victor Adeola[σ], Olusola Ademola Olaniyi[ρ] & Oladeji Aderibigbe Ajani[ω]

ABSTRACT

The study investigates the in-vitro antibacterial activity of greenly synthesized silver nanoparticles from Piper guineese leave (PgMLE) and seed (PgMSE) methanol extracts. The greenly synthesized silver nanoparticles from leave (PgMLEAgNPs) and seed (PgMSEAgNPs) extracts were characterized using UV-visible spectroscopy, FTIR, SEM, TEM, XRD, EDX, and TGA, and the in-vitro antibacterial activity of the extracts and nanoparticles against test pathogens from gastrointestinal tracts was evaluated. The PgMLE and PgMSE bio-reduced silver nitrate solution for the biosynthesis of PgMLEAgNPs and PgMSEAgNPs. The nanoparticles had the highest Surface plasmon resonance peaks at 500 nm. Functional groups such as alcohols, phenols, alkenes or alkynes, nitriles, ketones, aldehydes, or esters were identified as indicative of biomolecules present within PgMLEAgNPs, and PgMSEAgNPs. PgMLEAgNPs and PgMSEAgNPs were spherical flakelike and aggregated particles respectively with 15 nm in size, TEM shows the spherical shape nanoparticles. The nanoparticles were crystalline in nature and silver had the highest intensity as shown by XRD and EDX analysis. PgMLEAgNPs and PgMSEAgNPs exhibited varied antibacterial activity against the test pathogens. The antibacterial activity ranged from 2.00 to 18.00 mm in which E. coli had the highest susceptibility to PgMSEAgNPs compared to PgMLEAgNPs. The nanoparticles had better antibacterial efficacy against the test pathogens compared to the Piper guineense leaves and seed extracts. In conclusion, Piper guineense leave and seed extract nanoparticles had profound antibacterial activity against bacteria from GIT which makes them a candidate for biomedical application.

Keywords: Piper guineense methanol extracts, antibacterial activity, Silver nanoparticles, Gastrointestinal Tracts, Pathogens.

Author α σ: Department of Microbiology, University of Ibadan, Ibadan, Oyo State, Nigeria.
ρ: Department of Mathematics and Computer Science, University of North Carolina, Pembroke, USA.
ω: Federal Medical Center, Old N. North Carolina HWY 75, Buurner, NC 27509.

I. INTRODUCTION

The gastrointestinal tract is the site of the most well-known infectious diseases. These illnesses are brought on by bacterial infections and have long presented a challenge to the medical research community. Since the majority of people in developing nations live in poverty and infectious diseases are the main cause of morbidity and mortality, the development of new antimicrobials is of paramount importance (Look *et al.*, 2010). Up to date, various threats posed by infectious diseases that cannot be effectively prevented or treated with antibiotics, and antibiotic resistance as a result of numerous factors is of global health concern (Chadwick *et al.*, 2010).

Antimicrobial agent use has occasionally resulted in drops in morbidity and death (Huh and Kwon, 2011). Hydrophobic active plant components are increasingly being nanonized through trapping or encapsulation within inorganic or organic nanocarrier molecules, a technique known as nanotechnology. Nanotechnology is defined as the science of creating, utilizing, and applying nanostructures or nanomaterials, as well as examining the connections between different material qualities and their nanoscale dimensions (Siddiqi and Husen, 2017). It was discovered that nanomedicines created using this method can release active medicinal ingredients continuously from Nano carrier molecules, maintaining the medication's potency for an extended amount of time (Sarmukaddam *et al.*, 2010). Nanoparticles can be defined as small particles ranging in size from 1-100 nm and are undetectable by the human eyes.

As a result of the strong antioxidant action, medicinal plant extracts are employed as nano stabilizers and nanocarriers to decrease metal salts and oxides of Ag, Au, Cu, and Zn to metallic nanoparticles (NPs), which may be produced in a green synthetic form and have antibacterial properties (Dubey *et al.*, 2010; Zamare *et al.*, 2016; Mali *et al.*, 2020; Jayachandran *et al.*, 2021). Modern technologies use metallic nanoparticles because of their distinctive morphologies, surface Plasmon features, and intriguing physicochemical properties, among other things (Agnihotri *et al.,* 2014). According to Jamiu and Bello (2018), silver has long been utilized and recognized for its antibacterial activity. Due to their size, shape, and structure, as well as their huge surface-to-volume ratio, silver nanoparticles (AgNPs) have unique and more effective antibacterial properties when reduced to their nano-form (Rafique *et al.*, 2017). AgNPs are among the most widely used nanoparticles that show a broad spectrum of antibacterial activity (Ghodsieh *et al.,* 2016). The development of new bioactive antimicrobial compounds from plant extracts and the formulation of novel antimicrobial nanoparticles (NPs) using plant extracts as a bio-reducing agent can be considered as an adjuvant treatment or an alternative to antibiotics that can be used as therapeutics against gastrointestinal pathogens.

Piper guineense from the family Piperaceae is grown in Nigeria and is commonly known as Iyere in Yoruba and Uziza in Igbo. This plant yields fruit that is used as black pepper, Benin pepper, Ashanti pepper, or West African pepper (Faluyi, 2020). Iyere is regarded as the "king of all spices," and because of the presence of various bioactive compounds such as piperine, phenolic acids, and antioxidants, it has been employed in Ayurvedic medicine for thousands of years (Faluyi, 2020). It is used as a seasoning agent, for cosmetic, therapeutic, and insecticidal uses (Anyanwu and Nwosu, 2014 and Ogbunugafor *et al.,* 2017). The plant possesses antioxidant, anticonvulsant, anti-inflammatory, and neuropharmacological activities (Oyemitan *et al.,* 2015 and Salehi *et al.,* 2019).

To develop novel therapeutic antimicrobials using plant extracts as a nanocarrier to combat antibiotic resistance and gastroenteritis, hence a need for the use of *Piper guineense* extracts for the green synthesis of a novel drug. The study aimed at the biosynthesis of silver nanoparticles using methanol extract of *Piper guineense* seed and leaf as a bio-reducing and nanocarrier, characterization of the nanoparticles, and in-vitro determination of the antibacterial potential of the extracts and their nanoparticles against clinical isolates from gastrointestinal tracts.

II. MATERIALS AND METHODS

2.1 Collection of Plant Material and Cultures

Uziza (*Piper guineense*) seed and leaf used for this study were obtained from Gbogan market, Osun state, Nigeria. The plants were identified and authenticated at the Herbarium unit, Department of Botany, University of Ibadan. Clinical cultures (*E.coli, Klebsiella pneumoniae, and Shigella* sp.)

previously isolated from Gastrointestinal Tracts were collected from Microbiology Unit, University Teaching Hospital, University of Ibadan, Ibadan, Oyo state, Nigeria.

2.2 Sample Preparation and Extraction for Seed and Leave samples

Piper guineense seeds were thoroughly rinsed with distilled water, dried, and ground into fine powder. Five grams of powdered seed samples were weighed into an Erlenmeyer flask containing 50 mL of methanol. The mixture was heated for 15–20 min at 80 °C in a water bath. After boiling, the extract was filtered through Whatman's filter paper (No. 1) to remove any coarse material. A rotary evaporator operating at low temperatures and reduced pressure was used to concentrate the filtrate. The extract was then stored in an airtight container at 4°C in the refrigerator before use (Rautela *et al.,* 2019).

The leaves were cleaned with sterile water, dried, and then chopped into little pieces with a blender to prepare the plant crude extract. Then 50 g of each leaf sample was heated at 80°C in 250 ml of sterile water in a 500 mL Erlenmeyer flask for 30 min. After that, Whatman No. 1 was used to filter the crude leaf extracts, and they were kept at 4°C (Velu *et al.*, 2017).

2.3 Green Synthesis of Silver Nanoparticles Using Piper guineense Methanol Extracts

The production of silver nanoparticles was done according to the method of Rizwana *et al.* (2022). The crude extract from seeds and leaves was used for the biosynthesis of silver nanoparticles. 100 mL of 1 mM of the aqueous solution of silver nitrate ($AgNO_3$) was prepared in 250 mL Erlenmeyer flasks. The extracts were dissolved in Dimethyl Sulphur oxide (DMSO) at a concentration of 20 mg/mL. From the dissolved extracts, 10 mL each was mixed with 40 mL of silver nitrate ($AgNO_3$) solution in different 250 mL Erlenmeyer flasks for bio-reduction of the silver nitrate ($AgNO_3$) to silver (Ag^+) ions. The mixtures were then exposed to sunlight for bio-reduction of the $AgNO_3$ by the extracts to Ag^o ions. This formation of ions will form a deep brown color.

2.4 Characterization of Biosynthesized Nanoparticles

2.4.1 UV–Visible Spectroscopy of the Biosynthesized Ag Nanoparticles

This was carried out to ascertain the biosynthesized silver nanoparticles' optical characteristics. The biosynthesized nanoparticles were diluted with 2mL of deionized water and measured for spectrum at regular intervals. To blank all spectra for background correction, deionized water was used. All samples were loaded into a 1cm path-length quartz cuvette for UV-Vis spectrometric readings and scanned between 200 and 800nm wavelength, having a resolution of 1 nm. The UV-visible spectra were recorded at different intervals of 24-72 hours (Sanchooli *et al.*, 2018).

2.5 Fourier Transform Infrared Spectroscopy (FT-IR) of the Biosynthesized Ag Nanoparticles

The biosynthesized nanoparticles were further characterized using FTIR (spectrometer model 8400, Shimadzu) to detect the various functional groups responsible for the reduction, capping, and stabilizing of silver nitrate to form silver ions. For the FTIR analysis, the dried biosynthesized AgNPs were added to FTIR-grade potassium bromide (KBr) in 1: 30 ratios, and in transmittance mode, the spectrum was recorded at a resolution of 4 cm^{-1} and the spectrum was observed in the wave number range of 350-4,000 cm^{-1} (Mondal *et al.,* 2020).

2.6 Scanning Electron Microscopy (SEM) of the Biosynthesized Ag Nanoparticles

Scanning electron microscopy was employed to evaluate the Ag nanoparticles' surface structure. After 72 hours of reaction, the colloidal sample AgNPs was centrifuged at 4,000 x g for 15 minutes. The supernatant was discarded while the precipitate was dispersed in sterile water, followed by

centrifugation. This process was repeated thrice following a 30 minutes sonication to create a suspension, a drop of the nanoparticle solution was applied to a copper grid coated with carbon. The sample was kept under a lamp until completely dried and subjected to SEM analysis using a Phenom ProX Scanning Electron Microscope (Alkammash, 2017).

2.7 Transmission Electron Microscopy (TEM) of the Biosynthesized Ag Nanoparticles

TEM is used to study the sizes of the biosynthesized AgNPs from Uziza methanolic leaf and seed extracts. The biosynthesized nanoparticles were centrifuged at 4,000 x g for 15 minutes after 72 hrs of reaction. The sediments were dispersed in sterile water and centrifuged after the supernatant was discarded. A tiny droplet of the pellets was spread out on a copper grid coated in carbon and let to dry. TEM analysis was performed by using JOEL JCM-7000 instrument operated at an accelerating voltage of 15kV with a resolution of 0.23 nm (Gericke and Pinches, 2006).

2.8 X-ray diffraction (XRD) of the Biosynthesized Ag Nanoparticles

XRD was used to determine the crystalline nature of the greenly synthesized nanoparticles. The XRD pattern obtained from Rigaku D/Max-IIIC PW 1800 X-ray diffractometer at 2θ ranges from 4 to 70°. The sample for XRD measurement was prepared by casting the powder of silver nanoparticles on a glass slide and subsequently airdrying it under ambient conditions. The pattern was recorded by CuKα radiation with λ of 0.15 Å at a voltage of 40 kV and current of 20 mA with a scan rate of 10°/min (Adebayo-Tayo *et al.,* 2019 and Rautela *et al.,* 2019).

2.9 Energy Dispersive X-ray (EDX) of the Biosynthesized Ag Nanoparticles

EDX was used to determine the elemental composition of nanoparticles. The biosynthesized nanoparticles were centrifuged at 4,000 x g to obtain the pellet. The pellet was allowed to dry. A 100 nm thick section of the pellet was placed on the grid and analyzed using the Rigaku instrument model NEXCG. A pure selenium standard was used for calibration, and then a working curve was selected according to the sample. The sample was then tested and the result was outputted (Nayak *et al.*, 2014).

2.10 Thermogravimetric Analysis (TGA)

TGA was used to examine the thermal-induced degradation of the biosynthesized silver nanoparticles and this was conducted using Perkin-Elmer Thermogravimetry Analyzer Pyris 2. The analysis was carried out on approximately 25mg of samples at the temperature range of 35-1000 °C at a constant heating rate of 5 °C/min in a static air atmosphere.

2.11 Antibacterial Activities of the plant extracts and the biosynthesized Silver Nanoparticles (SNPS) against some GIT pathogens.

The test pathogens were maintained on an agar slant and stored at 4°C until use. The antibacterial activity of the extracts, and nanoparticles were determined using the agar well diffusion method. The extracts were dissolved in DMSO to form a concentration of 20 mg/mL. $AgNO_3$, DMSO, and Streptomycin were used as controls. The turbidity standard of each of the typed strains was prepared and compared to the McFarland standard. With sterile swab sticks, lawns of the standard were made on Nutrient Agar (NA) and a sterile cork-borer of diameter 6 mm was used to make holes in the plates. A micropipette machine was used to dispense 200 µL of the crude extracts and their SNPs into respective labeled wells. The plates were incubated at 37°C for 24 hours and the zones of inhibition (ZOI) (mm) were measured and recorded.

III. RESULTS

Silver nanoparticles were biosynthesized from the methanolic extract of *Piper guineense* seed and leaf. Figure 1 shows the visual observation of the biosynthesized nanoparticles. Color changes from green to brown after exposure to sunlight for bio-reduction of the $AgNO_3$ indicating the formation of AgNPs.

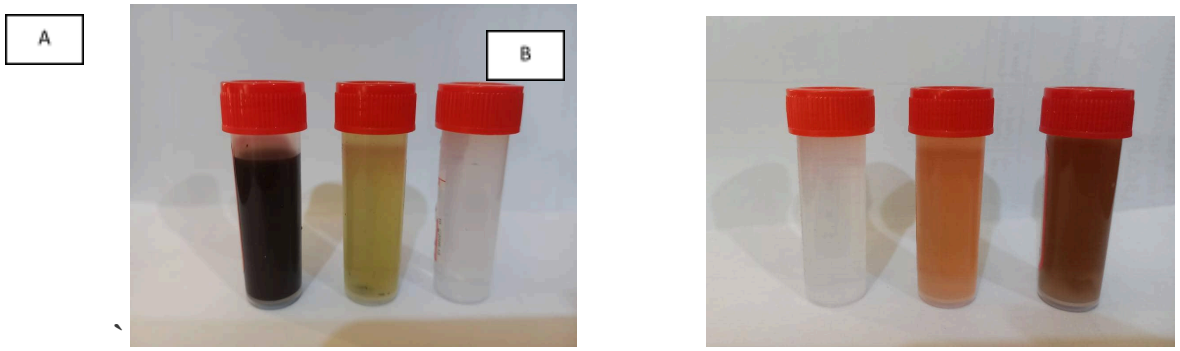

Key: A: 1- PgMSEAgNPs; 2-$AgNO_3$ + PgMSE and 3 - $AgNO_3$: B: 1 - $AgNO_3$, 2-$AgNO_3$ + PgMLE, **3-** PgMLEAgNPs

Figure 1a and b: Visual Observation of a) PgMSEAgNPs and b) PgMLEAgNPs

The biosynthesized AgNPs were monitored by measuring the metal ion reduction by periodically measuring their absorbance at different wavelengths ranging from 200 nm to 900 nm using a UV-Vis spectrophotometer. UV-vis spectra of the biosynthesized AgNPs are shown in Figures 2a and b. The PgMSEAgNPs had an absorption maximum within 400 nm to 500 nm with the highest surface Plasmon Resonance (SPR) peak absorbance of 1.889, 2.211, and 2.102 OD observed after 24, 48, and 72 hrs respectively at 500 nm wavelength which indicates the production of AgNPs. The PgMLEAgNPs had an absorption maximum within 400 nm to 500 nm with the highest surface Plasmon Resonance (SPR) peak absorbance of 1.970, 2.369, and 2.223 OD observed after 24, 48, and 72 hrs respectively at 500 nm wavelength which indicates the production of AgNPs.

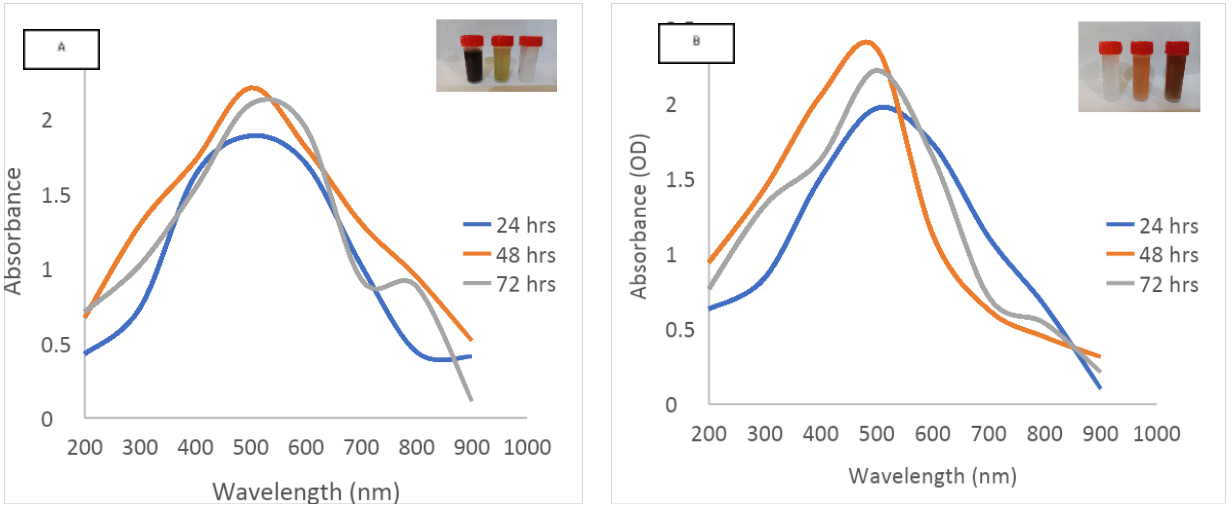

Figure 2a and b: UV-Visible Spectra of a) PgMSEAgNPs and b) PgMLEAgNPs

The FTIR analysis was performed to identify the potential biomolecules in PgMSEAgNPs and PgMLEAgNPs which are responsible for the bio-reduction and capping of the biosynthesized nanoparticles by characterizing the functional groups present on the surface of the nanoparticles. Figure 3a and b shows the FTIR spectrum of the biosynthesized nanoparticles and the spectra were measured at wave number 4000 – 350 cm^{-1}. The spectra for PgMSEAgNPs showed 12 major absorption peaks which indicates the presence of the different functional groups. The peak observed in the higher

energy region of intense absorption is 3757.00 and 3436.00 cm^{-1} which is characteristic of the stretching vibrations of O-H bonds in hydrogen-bonded hydroxyl (OH) groups, such as in alcohols or phenols. The peak at 2926.54, and 2859.80 corresponds to the asymmetric stretching vibrations of C-H bonds in aliphatic hydrocarbons. It is typical of alkanes and similar compounds. The peak at 2374.66 suggests the presence of a highly polarized bond, such as a triple bond (e.g., C≡N or C≡C) or nitriles. The peak at 2000.00 indicates the presence of carbon-carbon multiple bonds, like C=C double bonds in alkenes or alkynes. The peak at 1878.21 is often associated with carbon-carbon multiple bonds or possibly nitriles (C≡N) while the peak at 1630.66 indicates the presence of carbonyl groups (C=O) in compounds, such as ketones, aldehydes, or esters. The peak at 1054.09 is often related to C-O stretching vibrations in alcohols, ethers, or esters. The peak at 778.34 and 683.13 indicates the out-of-plane bending vibrations of aromatic (benzene-like) C-H bonds. The peak at 451.36 is in the fingerprint region, and this indicates the existence of metal oxide. These functional groups identified are indicative of biomolecules present within PgMSEAgNPs.

The spectra for PgMLEAgNPs showed 13 major absorption peaks which indicates the presence of the different functional groups. The peak observed in the higher energy region of intense absorption is 3868.00, 3752.23, and 3445.00 which is characteristic of the stretching vibrations of O-H bonds in hydrogen-bonded hydroxyl (OH) groups, such as in alcohols or phenols. The peak at 2927.76 corresponds to the asymmetric stretching vibrations of C-H bonds in aliphatic hydrocarbons. It is typical of alkanes and similar compounds. The peak at 2375.83 suggests the presence of a highly polarized bond, such as a triple bond (e.g., C≡N or C≡C) or nitriles. The peak at 1997.76 indicates the presence of carbon-carbon multiple bonds, like C=C double bonds in alkenes or alkynes. The peak at 1877.00 is often associated with carbon-carbon multiple bonds or possibly nitriles (C≡N) while the peak at 1631.73 indicates the presence of carbonyl groups (C=O) in compounds, such as ketones, aldehydes, or esters. The peak at 1056.00 is often related to C-O stretching vibrations in alcohols, ethers, or esters. The peak at 780.48 and 685.36 indicates the out-of-plane bending vibrations of aromatic (benzene-like) C-H bonds. The peak at 451.65 is in the fingerprint region, and this indicates the existence of metal oxide, and the peak at 373.47 is associated with the bending vibrations of strong covalent bonds or lattice vibrations in inorganic compounds. These functional groups identified are indicative of biomolecules present within PgMLEAgNPs.

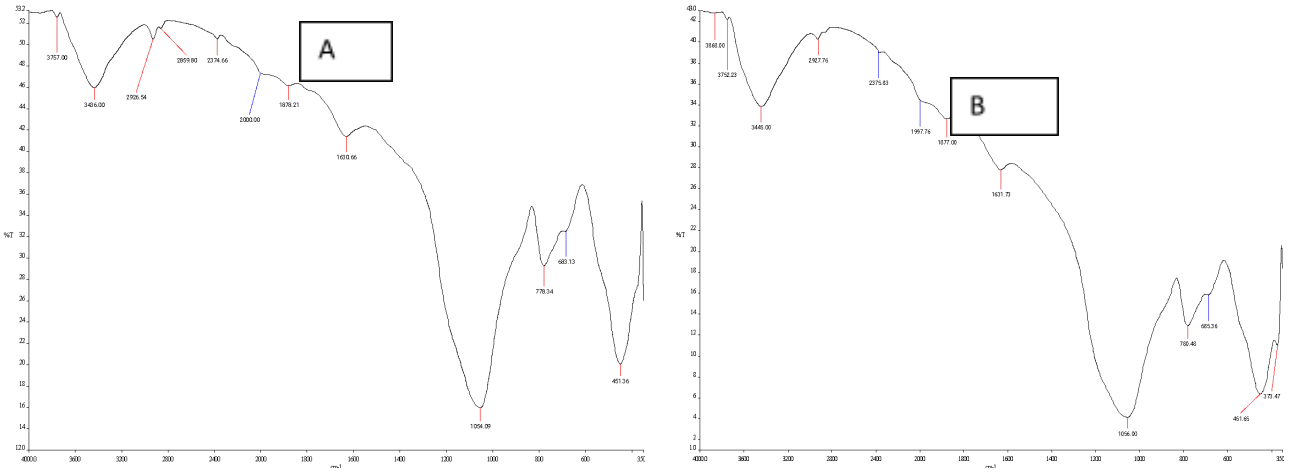

Figure 3a and b: Fourier Transform Infrared Spectroscopy (FTIR) of a) PgMSEAgNPs and b) PgMLEAgNPs

Scanning Electron Microscope (SEM) was used to observe the shape and surface characteristics of the biosynthesized nanoparticles. Figure 4a and b shows the scanning electron micrograph of the biosynthesized PgMSEAgNPs and PgMLEAgNPs. PgMSEAgNPs had an aggregated surface however there were variations in their morphology which is not unusual for biosynthesized nanoparticles shape while PgMLEAgNPs were spherical and flakelike in shape. Figure 4c and d shows the 3D image of PgMSEAgNPs and PgMLEAgNPs. Both 3D SEM images of the biosynthesized AgNPs revealed the particles to have nano-sized 15 nm.

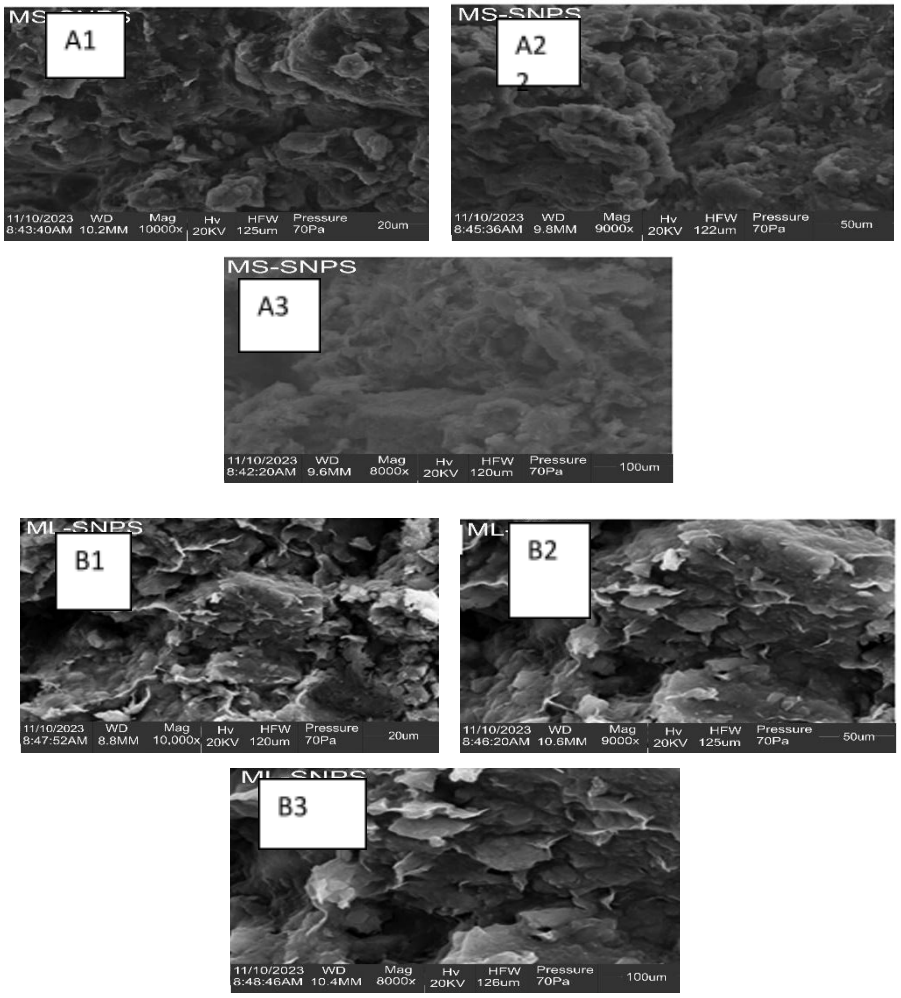

Figure 4a and b: Scanning Electron Microscopy (SEM) of a) PgMSEAgNPs and b) PgMLEAgNPs

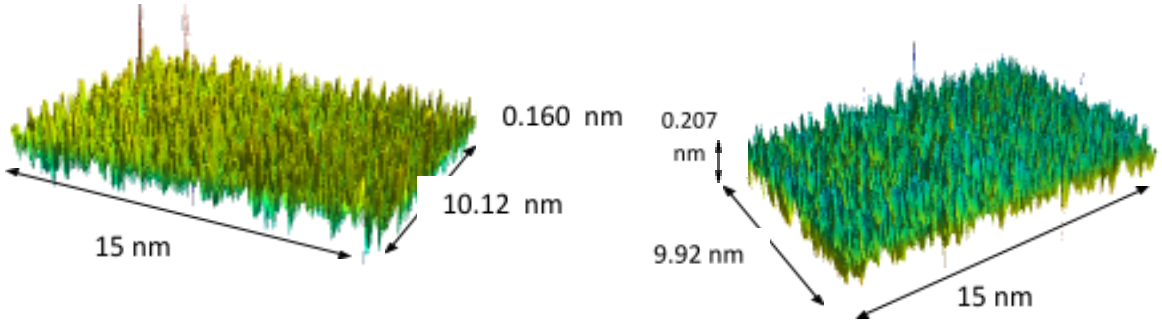

Figure 4c and d: 3D image of a) PgMSEAgNPs and b) PgMLEAgNPs.

Transmission Electron Microscope (TEM) was used to observe the shape and size of the biosynthesized nanoparticles. Figure 5a and b shows the Transmission electron micrograph of the biosynthesized PgMSEAgNPs and PgMLEAgNPs and that the particles are both nanoscale and uniform. PgMSEAgNPs and PgMLEAgNPs had spherical forms and the size ranged from 1.32 to 5.32 nm.

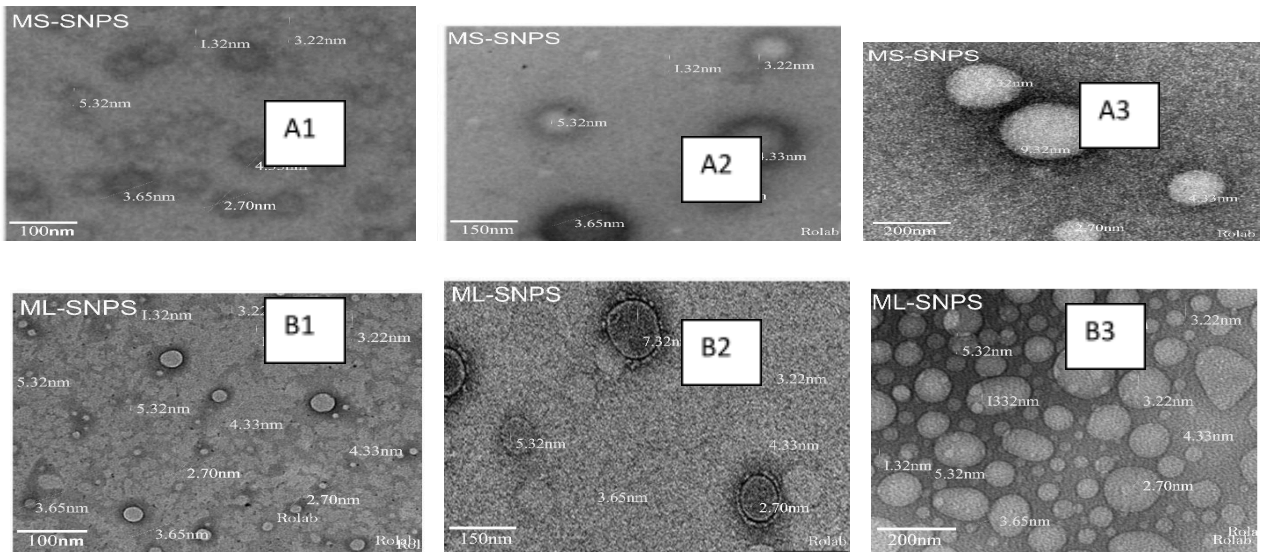

Figure 5a and b: Transmission Electron Microscopy (TEM) of a) PgMSEAgNPs and b) PgMLEAgNPs

X-ray diffraction was used to examine the size, crystalline makeup, purity, and quality of the nanoparticle. Figure 6a and b shows the X-ray diffractogram (XRD) pattern for PgMSEAgNPs and PgMLEAgNPs. The diffraction highs 2θ = 26.5, 32.4, 35.6, 36.4, 47.4, 56.3, 63.4, 67.2, and 67.3 are related to 005, 100, 002, 101, 102, 110, 103, 112, and 201 respectively for PgMSEAgNPs while the diffraction highs 2θ were 30.3, 34.5, 35.8, 46.5, 55.5, 63.2, 66.3, 68.6, 70.2, and 73.3 are related to 100, 002, 101, 102, 110, 103, 200, 112, 201, and 202 respectively for PgMLEAgNPs. The biosynthesized nanoparticles were crystalline in nature.

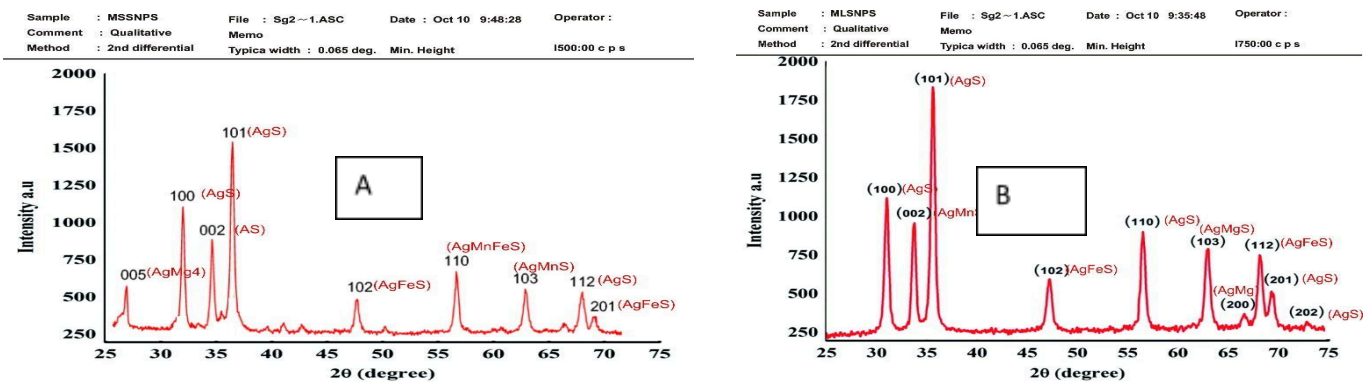

Figure 6a and b: X-ray Diffraction of PgMSEAgNPs and PgMLEAgNPs

The elemental analysis of PgMSEAgNPs and PgMLEAgNPs was revealed using the Energy X-ray Spectroscopy (EDX) which is shown in Figure 7a and b. The findings of EDX show that the Silver (Ag) atoms present have a significant signal. Further peaks that were seen include C, O, K, S, and Si for PgMSEAgNPs while C, O, Na, S, and Si for PgMLEAgNPs. From the result, silver (Ag) has the highest intensity of 65.20 % and 64.50 % for PgMSEAgNPs and PgMLEAgNPs respectively.

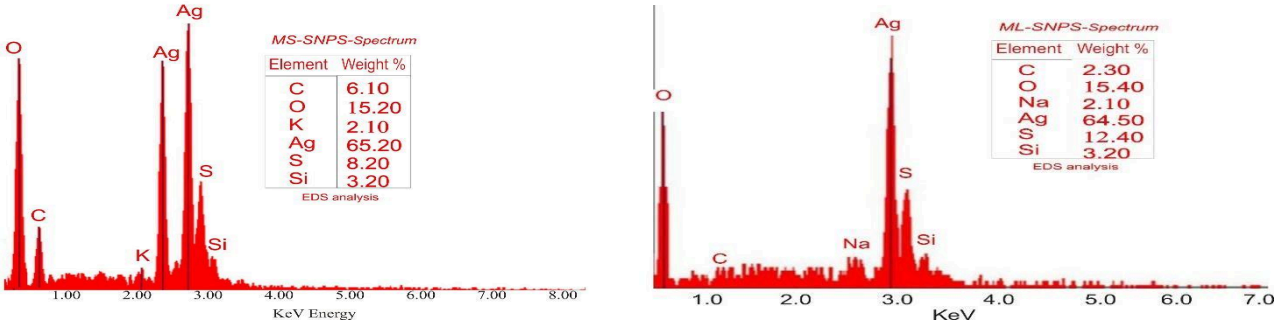

Figure 7a and b: EDX analysis of a) PgMSEAgNPs and b) PgMLEAgNPs

The thermal stability of PgMSEAgNPs and PgMLEAgNPs about its weight was evaluated using Thermogravimetry (TGA). Figure 8a and b shows the TGA curve of weight loss that occurred in temperature region between 160 °C and 250 °C for PgMSEAgNPs and 200 °C and 300 °C for PgMLEAgNPs. There was little weight loss below 160 °C and above 250 °C for PgMSEAgNPs and little weight loss below 200 °C and above 300 °C for PgMLEAgNPs.

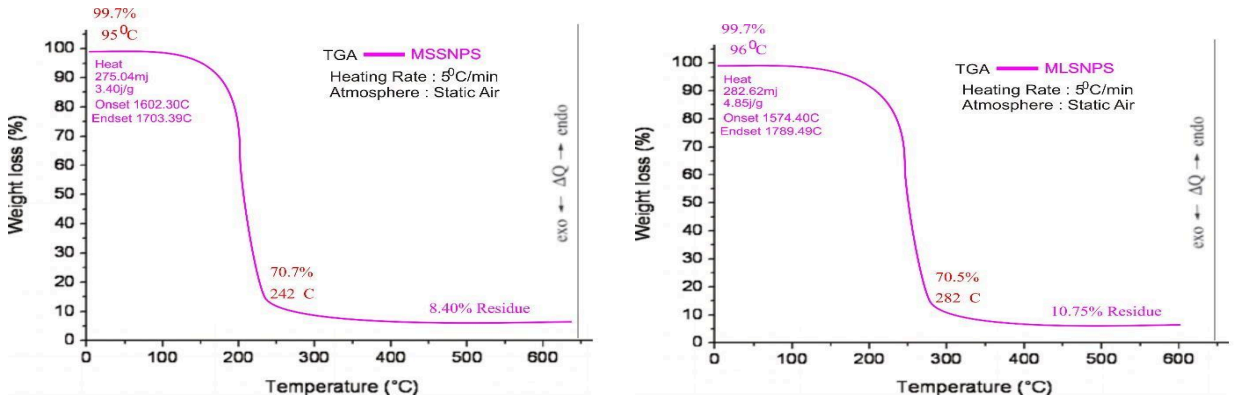

Figure 8a and b: TGA analysis of a) PgMSEAgNPs and b) PgMLEAgNPs

The antibacterial activity of the *P. guineense* methanol leaf and seed extract and its biosynthesized silver nanoparticle against test strains using the agar well diffusion method is shown in Table 1. The extracts and their nanoparticles have varied antibacterial activity against the test strains. The antibacterial activity ranged from 2.0 - 6.0 mm, 2.0 – 18.0 mm, 2.0 – 12.0 mm and 6.0 – 18.0 mm for Methanol leaf (ML), PgMLEAgNPs, Methanol Seed (MS) and PgMSEAgNPs respectively in which *E. coli* had the highest susceptibility (18mm) to PgMLEAgNPs. EC1 and U99 had the highest susceptibility (12mm) to MS and both UP_1 and EC11 had the highest susceptibility (18mm) to PgMSEAgNPs. It was observed that all extracts were 91.6% effective against the test pathogens except for PgMSEAgNPs which were 100% effective against all test strains. The result indicated that EC14 was resistant to both ML and PgMSEAgNPs, while EC21 was resistant to MS.

Table 1: Antimicrobial Activity of the methanol Piper *guineense* Extract and their Methanolic Silver Nanoparticle

Sample Code			Antibacterial Activity (mm) / Test pathogens									
	EC14	EC53	EC21	KLEB	EC114	EC1	SHI P45	UP1	EC104	EC11	U32	U99
ML	0	6	6	2	6	6	4	6	6	6	6	4
ML SNPs	0	8	14	6	2	8	8	8	8	12	0	18
MS	6	2	0	6	4	12	8	10	10	8	8	12
MS SNPs	12	10	12	6	14	12	12	18	6	20	0	8
Streptomycin	10	4	8	6	5	6	0	2	2	0	8	2
DMSO	0	0	0	0	0	0	0	0	0	0	0	0

KEY:

EC14	*Escherichia coli* Ec14		EC104	*Escherichia coli* EC104		EC1	*Escherichia coli* Ec1
EC53	*Escherichia coli* Ec53		EC11	*Escherichia coli* EC11		UP1	*Esxherichia coli* UP1
EC21	*Escherichia coli* Ec21		U32	*Escherichia coli* U32		KLEB	*Klebsiella pneumoniae*
EC114	*Esherichia coli* Ec114		U99	*Escherichia coli* U99		SHIP 45	*Shigella* sp P45

IV. DISCUSSION

The *P. guinesse* methanol leaves and seed extracts were able to bio-reduce silver nitrate for the biosynthesis of silver nanoparticles. Maxima absorbance peaks within 400 nm to 500 nm with increasing Surface Plasmon Resonance (SPR) peak as incubation time increased from 24 hrs to 48 hrs after which a decline set in at 72 hrs. A similar observation was reported by Cherian *et al.* (2018) in their study on "synthesis of biocompatible silver nanoparticles using leaf extract of *Piper nigrum*" which reported an absorbance peak at 420 nm specific for the AgNPs. Furthermore, it has been reported that absorption spectra of larger metallic colloidal dispersions can exhibit wide or additional bands in the UV–visible range due to the excitation of plasmon resonances or higher multipole plasmon excitations. The results from this study are consistent with previous studies reported by Jacob *et al.* (2012) and Otunola and Afolayan, (2018) on silver nanoparticles from *Piper longum* leaf extracts and aqueous extract of a spice blend formulation respectively. Also, according to Hemlata *et al.,* (2020) reported the presence of an absorbance peak at about 420 nm indicating the formation of AgNPs in the solution which may be as a results of surface plasmon resonance (SPR) electrons on the nanoparticle surface. The size, shape, and other individual metal particle characteristics, as well as the medium's dielectric qualities, all affect the SPR pattern and the inter-nanoparticle coupling interactions. The intensity of the SPR band increased with reaction time, indicating the synthesis of the AgNPs (Sikdar, 2023).

The FTIR analyses were to characterize AgNPs and to examine the possible bio-reducing functional groups present in PgMSEAgNPs and PgMLEAgNPs. The spectrum was captured from 350 cm^{-1} to 4000

cm^{-1}. The FTIR result of this study was in agreement with the report of Krishnan *et al.* (2016) on silver nanoparticles from *Piper nigrum* concoction. Similar peaks which indicated the same functional groups as indicated in this study were reported. However, the c=c stretch indicating the presence of alkenes was not recorded by Krishnan *et al.,* (2016). Complete suppression of iodo compounds OH group out of plane bending (521 and 565) may be due to the addition of silver nitrate, which means the complete reduction and stabilization of the silver nanoparticles. This is in agreement with this study at 451.65 and 373.47 for PgMLEAgNPs while 451.36 for PgMSEAgNPs. The modulated transmittance percentage of ketone, fluoro compounds, and amine groups was confirmed as they play a vital role in the bio-reduction of silver nitrate to silver nanoparticles. The presence of these peaks demonstrated that plant secondary metabolites, including terpenoids, flavonoids, glycosides, phenols, and tannins, as well as functional groups like aldehyde, carboxylic acid, and others, coated the nanoparticles. The presence of these groups is due to the stability of the nanoparticles (Bagherzade *et al.,* 2017).

The SEM analysis identified the nano-size and shape of PgMSEAgNPs and PgMLEAgNPs. The shape of the PgMSEAgNPs was not clear because they are aggregated. Due to the drying process, the aggregation may be observed. Adebayo-Tayo *et al.* (2019) observed a similar situation in their work on the rapid synthesis and characterization of gold and silver nanoparticles using exopolysaccharides and metabolites of *Wesiella confusa*. They concluded that sample preparation including drying can affect the shape and size of SNPs (Adebayo-Tayo *et al.,* 2019). The flake-like shape of PgMLEAgNPs was similar to the report Guo *et al.* (2021) on "Shape-controlled synthesis of flake-like $FeNi_3$ nanoparticles based on sodium lignosulfonate". Endah *et al.* (2022) reported a mixture of spherical and flake-like shapes for ZnO nanoparticles.

Using the XRD pattern the size of crystals was investigated and the crystallite size of silver nanoparticles for PgMSEAgNPs and PgMLEAgNPs was about 54 nm and 38 nm respectively. The XRD pattern thus clearly indicated that the AgNPs organized by the reduction of Ag+ ions by the aqueous extract of *Piper guineense* were crystalline in nature. Presence of these peaks was due to seed and leave extract which contains organic compounds and is responsible for the reduction of silver ions and stabilization of resultant nanoparticles. This result is similar to Giri *et al.,* (2022) as they report the average crystalline size of silver nanoparticle synthesized to be approximately 35 The elemental composition of the biosynthesized nanoparticles was analyzed using EDX spectroscopy. EDX analysis of the PgMSEAgNPs and PgMLEAgNPs shows that silver had the highest peak at 3 keV which indicates that Silver (Ag) is the main element present. The presence of other elements may be as a result of the residual phytoconstituents of *Piper guineense* acting as a capping agent on the surface of the nanoparticles or contaminants introduced into the sample during handling. The results of EDX spectroscopy support the results of UV-visible spectrophotometric analysis, confirming the formation of AgNPs by methanol extract of *P. guineense*. The EDX result in this study is similar to the findings of Adeleye *et al.* (2023) for *Ehretia cymosa* silver nanoparticles. When compared to SNPs from aqueous extract, SNPs had a greater absorption peak and element concentration by weight. This also agrees with the results of Maloma *et al.* (2023) on *T. polyzona* Laccase-Mediated Silver Nanoparticles. The silver nanoparticles show a characteristic strong signal peak at 3 keV as a result of the surface plasmon resonance. Additionally, other signals although weak, indicate the presence of C, O, S, and Si and these elements may have played a vital role in the stability and reduction of the nanoparticles. This agrees with the report of Adebayo-Tayo *et al.* (2022).

The Thermogravimetric analysis (TGA) of the synthesized nanoparticles revealed the thermal stability of the AgNPs synthesized. According to the TGA curve, the study weight loss was consistent and occurred in the temperature range of 160 °C and 250 °C (70.7%) for PgMSEAgNPs and 200 °C and 300 °C (70.5%) for PgMLEAgNPs. The loss was due to the decomposition and evaporation of phytochemicals/biomolecules on the surfaces of the silver nanoparticles as surface stabilizing/capping

agents for both AgNPs synthesized. A closely similar result was reported by Zahoor *et al.* (2022) on *Rhynchosia capitata* leaf extract silver nanoparticles. A single weight loss between the temperature range 40 to 80 °C was observed which was due to the elimination of moisture contents from the NPs caused the sample's weight to decrease and the capping agent being organically decomposed rapidly with the increase in temperature and resulted in abrupt mass loss. Also, Hemali and Sumitra (2020) had a similar report on silver nanoparticles using *Ziziphus nummularia* leaf extract. They reported similar weight loss of AgNPs 100 °C to 800 °C which was due to thermal decomposition of plant bioorganic compounds absorbed on the surface of nanoparticles.

The result indicated that silver nanoparticles have considerably more antibacterial effects compared to leaf and seed extract of the plant. This observation conforms to the finding of Ghodsieh *et al.* (2017) on silver nanoparticles from aqueous extract of saffron (*Crocus sativus* L.) wastages. They reported a significant antibacterial effect of the nanoparticles against *some test pathogens* and concluded that it can be used in biomedical applications. This also agreed with the work of Loo *et al.* (2018) who reported that the AgNPs showed antibacterial activity against Gram-negative foodborne pathogens.

V. CONCLUSION

In this study, methanol extract of *Piper guineense* leaf and seed bio-reduced silver nitrate for nanoparticles biosynthesis and act as a nanocarrier for the *P. guineense* seed and leave bioactive chemicals with varied antibacterial activity against the test pathogens from gastrointestinal tract. The biosynthesized silver nanoparticles from methanol leaf and seed *Piper guineense* extract have more potent antimicrobial activity compare to the extracts. Therefore, further studies are needed to fully characterize the toxicity and the modes and mechanisms of antimicrobial action and antioxidant activity of these biomolecules and the particles.

Data Availability

The data that support the findings of this study are available on request.

Conflicts of Interest

The authors have no competing interests to declare regarding this article.

Authors' Contributions

The conception, design, and execution of the study were a collaborative effort by all authors. Bukola Christianah Adebayo-Tayo, Folarin Victor Adeola, Olusola Ademola Olaniyi and Oladeji Aderibigbe Ajani performed material preparation, data collection, and analysis. The initial manuscript draft was written by Folarin Victor Adeola, and all authors provided feedback on previous versions. The final manuscript was read and approved by all authors.

Acknowledgments - Not applicable

Funding

The research was self-funded by the authors.

REFERENCES

1. Adebayo-Tayo, B.C., A. Salaam, A. Ajibade (2019). Green synthesis of silver nanoparticle using *Oscillatoria* sp. extract, its antibacterial, antibiofilm potential and cytotoxicity activity. *Journal of Heliyon*. **5**: 10-25.

2. Adebayo-Tayo, B. C., S. O. Borode, S. O. Alao (2022). *In–Vitro* Antibacterial and Antifungal Efficacy of Greenly Fabricated *Senna alata* Leaf Extract Silver Nanoparticles and Silver Nanoparticle-Cream Blend. *Period. Polytech. Chem. Eng*. **66**: 248–260.
3. Adeleye, O.A., K. O. Aremu, H. Iqbal, M. O. Adedokun, O. A. Bamiro, O. L. Okunye, M. N. Femi-Oyewo, K. O. Sodeinde, S. Z. Yahaya, A. O. Awolesi (2023). Green Synthesis of Silver Nanoparticles Using Extracts of *Ehretia cymosa* and Evaluation of Its Antibacterial Activity in Cream and Ointment Drug Delivery Systems. *J. Nanotechnol.* https://doi.org/10.1155/2023/2808015.
4. Agnihotri, S., S. Mukherji, S. Mukherji (2014). Size-controlled silver nanoparticles synthesized over the range 5 – 100 nm using the same protocol and their antibacterial efficacy. *Adv. Res*. 3974-3983
5. Ajileye, O.O., M. A. Aderogba, E. M. Obuotor, E. O. Akinkunmi (2015). Isolation and characterization of antioxidant and antimicrobial compounds from *Acacardium occidentale* L. (Anacardiaceae) leaf extract. *J. King Saud Univ. Sci.* **27**: 244-252
6. Alkammash, N. M. (2017). Synthesis of Silver Nanoparticles from Artemisia Sieberi and Calotropis Procera Medical Plant Extracts and Their Characterization using SEM Analysis. *Biosci. Biotechnol. Res. Asia*. **14(**2).
7. Anyanwu, C.U., G. C. Nwosu (2014). Assessment of the antimicrobial activity of aqueous and ethanolic extracts of *Piper guineense* leaves. *J. Med. P. Res*. **8**: 436–40.
8. Bagherzade, G., M. M. Tavakoli, M. H. Namaei (2017). Green synthesis of silver nanoparticles using aqueous extract of saffron (*Crocus sativus* L.) wastages and its antibacterial activity against six bacteria. *Asian Pac. J. Trop. Biomed*. **7**: 227–233.
9. Chadwick, S., C. Kriegel, M. Amiji (2010). Nanotechnology solutions for mucosal immunization. *Adv. Drug Deliv. Rev*. **62**: 394-407.
10. Cherian, T., T. Jamal, S. K. Yalla, R. Mohanraju (2018). One-pot green synthesis of biocompatible silver nanoparticles using leaf extract of *Piper nigrum*. *IJPBS*. **8**: 1082-1088.
11. Dubey, S. P., M. Lahtinen, H. Sarkka, M. Silanpaa (2010). Bioprospective of *Sorbus aucuparia* leaf extract in development of silver and gold nanocolloids. *Colloids Surf. B*. **80**: 26–33.
12. Endah, E.S., V. Saraswaty, D. Ratnaningrum, W. Kosasih, A. Ardiansyah, C. Risdian, P. Nugroho, S. E. Aji, H. Setiyanto (2022). Phyto-assisted synthesis of zinc oxide nanoparticles using mango (Mangifera indica) fruit peel extract and their antibacterial activity. *Environ. Earth Sci.* **1201:** 012081.
13. Faluyi, O. (2020). Take advantage of the health benefits of iyere (*Piper guineense*). https://punchng.com/take-advantage-of-the-health-benefits-of-iyere-piper-guineense/
14. Gericke, M., A. Pinches (2006). Biological Synthesis of Metal Nanoparticles. *Hydrometallurgy*. **83:** 132-140.
15. Ghodsieh, B., M. T. Maryam, H. N. Mohmmad (2016). Green synthesis of silver nanoparticles using aqueous extract of saffron (*Crocus sativus* L.) wastages and its antibacterial activity against six bacteria. *Asian Pac. J. Trop. Biomed*. **7**: 227-233.
16. Hemali, P., C. Sumitra (2020). Synthesis of silver nanoparticles using *Ziziphus nummularia* leaf extract and evaluation of their antimicrobial, antioxidant, cytotoxic and genotoxic potential (4-in-1 system). *Artif Cells Nanomed Biotechnol*. **49**: 354-366.
17. Hemlata, P. R. Meena, P. A. Singh, K. K. Tejavath (2020). Biosynthesis of Silver Nanoparticles Using *Cucumis prophetarum* Aqueous Leaf Extract and Their Antibacterial and Antiproliferative Activity Against Cancer Cell Lines. *ACS omega*. **5**: 5520–5528
18. Huh, A. J., Y. J. Kwon (2011). "Nanoantibiotics": a new paradigm for treating infectious diseases using nanomaterials in the antibiotics resistant era. *JCR*. **156**: 128-145.
19. Jacob, J.P.S., J. S. Finub, A. Narayanan (2012). Synthesis of silver nanoparticles using *Piper longum* leaf extracts and its cytotoxic activity against Hep-2 cell line. *Colloids Surf. B*. **91**: 212– 214

20. Jamiu, A.T., S. Bello (2018). Biosynthesis of Silver Nanoparticles using *Azadirachta indica* Leaf Extract and Assessment of its Antibacterial Activity on some Pathogenic Enteric Bacteria. *IJRDPL*. **5**: 25-31.
21. Jayachandran, A., T. R. Aswathy, A. S. Nair (2021). Green synthesis and characterization of zinc oxide nanoparticles using Cayratia pedata leaf extract. *Biochem. Biophys. Rep*. **26:** 100995.
22. Krishnan, V.l., G. Bupesh, E. Manikandan, A. K. Thanigai, S. Magesh, R. Kalyanaraman, M. Maaza (2016). Green Synthesis of Silver Nanoparticles Using Piper nigrum Concoction and its Anticancer Activity against MCF-7 and Hep-2 Cell Lines. *J. Antimicrob. Agents*. **2**: 1000123
23. Loo, Y.Y., Y. Rukayadi, M. Nor-Khaizura, C. H. Kuan, B. W. Chieng, M. Nishibuchi, S. Radu (2018). In Vitro Antimicrobial Activity of Green Synthesized Silver Nanoparticles Against Selected Gram-negative Foodborne Pathogens. *Front. microbiol*. **16**: 9
24. Look, M., A. Bandyopadhyay, J. S. Blum, T. M. Fahmy (2010). Application of nanotechnologies for improved immune response against infectious diseases in the developing world. *Adv. Drug Deliv. Rev*. **62:** 378-393.
25. Mali, S.C., A. Dhaka, C. K. Githala, R. Trivedi (2020). Green synthesis of copper nanoparticles using *Celastrus paniculatus* Wild leaf extract and their photocatalytic and antifungal properties. *Biotechnol. Rep*. **27:** e00518.
26. Maloma, R.M., B. C. Adebayo-Tayo, Y. A. Alli, P. O. Oladoye (2023). Synthesis and Characterization of *T. polyzona* and Laccase-Mediated Silver Nanoparticles: Antimicrobial and Printing Press Wastewater Treatment Efficiency. *Chem. Afr*. **6:** 2509–2521.
27. Mondal, A.H., D. Yadav, S. Mitra, K. Mukhopadhyay (2020). Biosynthesis of Silver Nanoparticles Using Culture Supernatant of *Shewanella* sp. ARYI and their Antibacterial Activity. *Int J Nanomed*. **15:** 8295-8307.
28. Nayak, B.K., N. Chitra, A. Nanda (2014). Efficacy of biosynthesized AgNPs from *Alternaria chlamydospore* isolated from indoor air of vegetable market. *Int. J. Pharm. Technol*. **6:** 1309-1314.
29. Ogbunugafor, H.A., C. G. Ugochukwu, A. E. Kyrian-Ogbonna (2017). The role of spices in nutrition and health: A review of three popular spices used in Southern Nigeria. *Food Qual. Saf*. **1**:171–85.
30. Otunola, G.A., A. J. Afolayan (2018). In vitro antibacterial, antioxidant and toxicity profile of silver nanoparticles green synthesized and characterized from aqueous extract of a spice blend formulation. *Biotechnol. Biotechnol. Equip*. **32:** 1-10.
31. Oyemitan, I. A., O. A. Olayera, A. Alabi, L. A. Abass, C. A. Elusiyan, A. O. Oyedeji, M. A. Akanmu (2015). Psychoneuropharmacological activities and chemical composition of essential oil of fresh fruits of *Piper guineense* (Piperaceae) in mice. *J. Ethnopharmacol*. **166:** 240–9.
32. Rafique, M., I. Sadaf, M. S. Rafique, M. B. Tahir (2017). A review on green synthesis of silver nanoparticles and their applications. *Artif Cells Nanomed Biotechnol*. **45:** 1272-1291.
33. Rautela, A., J. Rani, M. Debnath (2019). Green synthesis of silver nanoparticles from Tectona grandis seeds extract: characterization and mechanism of antimicrobial action on different microorganisms. *JAST*. **10:** 5.
34. Rizwana, H., M. S. Alwhibi, R. A. Al-Judaie, H. A. Aldehaish, N. S. Alsaggabi (2022). Sunlight-Mediated Green Synthesis of Silver Nanoparticles Using the Berries of *Ribes rubrum* (Red Currants): Characterisation and Evaluation of Their Antifungal and Antibacterial Activities. *Molecules*. **27**: 2186.
35. Salehi, B., Z. A. Zakaria, R. Gyawali, S. A. Ibrahim, J. Rajkovic, Z. K. Shinwari, T. Khan, J. Sharifi-Rad, A. Ozleyen, E. Turkdonmez (2019). *Piper* species: A comprehensive review on their phytochemistry, biological activities and applications. *Molecules*. **24**: 1364.
36. Sanchooli, N., S. Saeidi, H. K. Barani, E. Sanchooli (2018). In vitro antibacterial effects of silver nanoparticles synthesized using *Verbena officinalis* leaf extract on *Yersinia ruckeri*, *Vibrio cholera* and *Listeria monocytogenes*. *IJM*. **10:** 400-408.

37. Sarmukaddam, S., A. Chopra, G. Tillu (2010). Efficacy and safety of Ayurvedic medicines: recommending equivalence trial design and proposing safety index. *Int. J. Ayurveda Res.* **1:** 175–180.
38. Siddiqi, S.K., A. Husen (2017). Plant Response to Engineered Metal Oxide Nanoparticles. *Nanoscale Res. Lett.* **12**.
39. Sikdar, M (2023). Green synthesis, optimization and analyzing of silver nanoparticles encapsulated with *Syzygium aromaticum* extract: Evaluating antibacterial and photocatalytic properties. *Bioresour. Technol. Rep.* ***24:*** 101669.
40. Velu, M., J. H. Lee, W. S. Chang, N. Lovanh, Y. J. Park, P. Jayanthi, V. Palanivel, B. T. Oh (2017). Fabrication, optimization, and characterization of noble silver nanoparticles from sugarcane leaf (*Saccharum officinarum*) extract for antifungal application. *Biotech.* **7:** 1-9.
41. Zahoor, M., M. Nisar, I. S. Haq, M. Ikram, N. U. Islam, M. Naeem, A. Alotaibi (2022). Green synthesis, characterization of silver nanoparticles using *Rhynchosia capitata* leaf extract and their biological activities. *Open Chem.* **21**: 20220318
42. Zamare, M.S., S. S. Vutukuru, R. Babu (2016). Biosynthesis of nanoparticles from agro-waste: a sustainable approach. *Int. j. appl. Sci.* **1:** 85–92.

This page is intentionally left blank